

Comparative transcriptomic analysis reveals the cold acclimation during chilling stress in sensitive and resistant passion fruit (*Passiflora edulis*) cultivars

Yanyan Wu ¹, Weihua Huang ¹, Qinglan Tian ¹, Jieyun Liu ¹, Xiuzhong Xia ², Xinghai Yang ^{Corresp., 2}, Haifei Mou ¹

¹ Biotechnology Research Institute, Guangxi Academy of Agricultural Sciences, Nanning, Guangxi, CHINA

² Rice Research Institute, Guangxi Academy of Agricultural Sciences, Nanning, Guangxi, CHINA

Corresponding Author: Xinghai Yang

Email address: yangxinghai888@gxaas.net

Chilling stress (CS) is an important limiting factor for the growth and development of passion fruit (*Passiflora edulis*) in winter in south China. However, we still know little is known about how the passion fruit responds and adapts to CS. In this study, we performed transcriptome sequencing of Huangjinguo (HJG, cold-susceptible) and Tainong 1 (TN1, cold-tolerant) under normal temperature (NT) and CS conditions, and a total of 47,353 unigenes were obtained in 7 databases. Using differentially expressed unigenes (DEGs) analysis, 3,248 and 4,340 DEGs were identified at two stages, respectively. The Gene Ontology (GO) enrichment analysis showed that the DEGs were mainly related to protein phosphorylation, phosphorylation, membrane protein, and catalytic activity. In Kyoto Encyclopedia of Genes and Genomes (KEGG) pathway, the unigenes of plant-pathogen interaction, plant hormone signal transduction and fatty acid metabolism were enriched. Then, the 12,471 filtered unigenes were divided into 8 co-expression modules, and two of which were correlated with chilling acclimation. In the two modules, 32 hub unigenes were obtained. Furthermore, the unigenes related to chilling tolerance were validated using quantitative real-time PCR (RT-qPCR). This work was the first systematic study of the molecular mechanism of chilling tolerance in passion fruit. The results provide information for the development of passion fruit with increased chilling tolerance.

1 **Title: Comparative transcriptomic analysis reveals the cold acclimation**
2 **during chilling stress in sensitive and resistant passion fruit (*Passiflora edulis*)**
3 **cultivars**

4 Yanyan Wu¹, Weihua Huang¹, Qinglan Tian¹, Jieyun Liu¹, Xiuzhong Xia², Xinghai Yang^{2*},
5 Haifei Mou^{1*}

6 ¹Biotechnology Research Institute, Guangxi Academy of Agricultural Sciences, Nanning,
7 Guangxi 530007, China

8 ²Rice Research Institute, Guangxi Academy of Agricultural Sciences, Nanning, Guangxi 530007,
9 China

10 ***Corresponding author:** Xinghai Yang; **Department/Institute:** Rice Research Institute,
11 Guangxi Academy of Agricultural Sciences; **Address:** 174 East Daxue Road, Nanning, Guangxi
12 530007, China; **E-mail:** yangxinghai514@163.com; Tel: +867713244040; ORCID ID:
13 <https://orcid.org/0000-0002-3476-2578>.

14 ***Co-corresponding author:** Haifei Mou; **Department/Institute:** Biotechnology Research
15 Institute, Guangxi Academy of Agricultural Sciences; **Address:** 174 East Daxue Road, Nanning,
16 Guangxi 530007, China; **E-mail:** mhf@gxaas.net; Tel: +86771 3243531

17

18

19

20

21

22

23

24

25

26

27

28

29 Abstract

30 Chilling stress (CS) is an important limiting factor for the growth and development of passion
31 fruit (*Passiflora edulis*) in winter in south China. However, we still know little is known about
32 how the passion fruit responds and adapts to CS. In this study, we performed transcriptome
33 sequencing of Huangjinguo (HJG, cold-susceptible) and Tainong 1 (TN1, cold-tolerant) under
34 normal temperature (NT) and CS conditions, and a total of 47,353 unigenes were obtained in 7
35 databases. Using differentially expressed unigenes (DEGs) analysis, 3,248 and 4,340 DEGs were
36 identified at two stages, respectively. The Gene Ontology (GO) enrichment analysis showed that
37 the DEGs were mainly related to protein phosphorylation, phosphorylation, membrane protein,
38 and catalytic activity. In Kyoto Encyclopedia of Genes and Genomes (KEGG) pathway, the
39 unigenes of plant-pathogen interaction, plant hormone signal transduction and fatty acid
40 metabolism were enriched. Then, the 12,471 filtered unigenes were divided into 8 co-expression
41 modules, and two of which were correlated with chilling acclimation. In the two modules, 32 hub
42 unigenes were obtained. Furthermore, the unigenes related to chilling tolerance were validated
43 using quantitative real-time PCR (RT-qPCR). This work was the first systematic study of the
44 molecular mechanism of chilling tolerance in passion fruit. The results provide information for
45 the development of passion fruit with increased chilling tolerance.

46 **Key words** Passion fruit, Chilling stress, RNA-seq, WGCNA, Hub genes, RT-qPCR

47 Introduction

48 Passion fruit is a tropical and subtropical fruit tree that is widely planted in south China and its
49 fruit has an aromatic smell and high nutritional values. But passion fruit is susceptible to cold
50 stress in winter (Liu et al. 2017A), which can cause large economic loss.

51 Cold stress is one of the limiting factors for plant growth and development (Shi et al. 2018). In
52 plants, cold stress is classified into chilling stress (CS, 0-15 °C) and freezing stress (<0 °C)
53 (Yadav 2010; Shi et al. 2018). The cold environment can cause changes in the structure and

54 activity of proteins in plant cells, leading to altered enzymatic reactions such as photosynthesis
55 and respiration, and eventually leading to symptoms such as wilting and yellowing of plant
56 leaves (Hendrickson et al. 2006). When plants are in reproductive growth, cold stress can cause
57 damage of the plant reproductive organs, and the seed setting rate will be significantly reduced,
58 which will eventually affect crop yields and cause major losses to agricultural production. Plants
59 can gain resistance to low temperature, and this process is called cold acclimation.

60 The cold acclimation of plants includes changes in a variety of intracellular physiological and
61 biochemical processes. The most significant changes include the instantaneous increase of
62 calcium ion concentration (Carpaneto et al. 2007), growth cessation, decrease in tissue water
63 content, affect the plant hormones abscisic acid (ABA), brassinolide (BR), and gibberellin (GA),
64 causes fatty acid unsaturation and lipid peroxidation (Hara et al. 2003), changes in phospholipid
65 composition (Webb et al. 1994), and osmotic adjustment substances such as proline, betaine and
66 soluble sugar (Krasensky j 2012). The molecular mechanism of cold acclimation is that non-
67 freezing low temperature can induce plants to express a series of cold response proteins to help
68 plants resist freezing at low temperature. ICE (inducer of CBF expression)-CBF (C-repeat
69 binding factors)-COR (cold-regulated proteins) is thought to be one of the most important
70 defense pathways in plant against cold stress (Shi et al. 2018). CBF can regulate the expression
71 of COR by binding to the C-repeat/dehydration-responsive element (CRT/DRE) sequence that
72 resides in the promoter region of *COR* gene (Stockinger et al. 1997; Liu et al. 1998). ICE1 is
73 located upstream of *CBF*, and it is a MYC-like bHLH type transcription factor, which can bind
74 to the recognition site of *CBF3* promoter and regulate its expression (Chinnusamy et al. 2003)
75 Moreover, some CBF-independent transcription factors are involved in modulating COR
76 expression, and various transcription factors, including CAMTA3 (Doherty et al. 2009), ZAT12
77 (Vogel et al. 2005), and HY15 (Catalá et al. 2011), can regulate the expression of CBFs. Protein
78 phosphorylation also plays an important role in regulating the response of plants to low
79 temperature (Mann m 2003), and mitogen-activated protein kinase (MAPK) as an important
80 element in signal transmission (Zhao et al. 2017A).

81

82 Guangxi belongs to a tropical and subtropical monsoon climate. The coldest month in January
83 has an average daily temperature of 5.5°C to 15.2°C. The continuous low temperature in winter
84 affects the growth of passion fruit. However, no systematic study on the CS of passion fruit
85 has been reported. In this study, the RNA-seq was used to analyze gene expression during CS in
86 passion fruit cultivars Huangjinguo (HJG, cold-sensitive) and Tainong 1 (TN1, cold-tolerant).
87 The main aims are: (i) to analyze the gene expression profile of passion fruit during CS; (ii) to
88 explore the functions of differentially expressed unigenes (DEGs) (iii) to construct regulation
89 network of the interactions of chilling tolerance genes of passion fruit; (iv) to identify the hub
90 genes that affect the chilling acclimation of passion fruit.

91 **Materials and Methods**

92 **Plant materials**

93 HJG is introduced in the Bannahuangguo of Xishuangbanna Botanical Garden in Yunnan, and it
94 is a cold-sensitive accession, .TN1 comes from Taiwan, and it is a cold-resistant purple passion
95 fruit. The cutting seedling heights ranged from 29 to 38 cm, and the seedlings were transplanted
96 in Nanning experimental field (Guangxi, China, 22.85 °N, 108.26 °E) on May 25, 2019. The first
97 sampling time was November 25th, 2019, at 10 am in the morning, and the temperature was 25
98 °C. The second sampling time was January 18, 2020, at 10 am in the morning, and the
99 temperature was 7 °C. The fresh leaves of passion fruit were snap frozen in liquid nitrogen, and
100 then stored in -80 °C freezer. Each sample had three biological replicates. Under NT condition,
101 the three biological replicates of HJG, HJGA1, HJGA2 and HJGA3, are recorded as A1; the
102 three biological replicates of TN1 TN1A1, TN1A2 and TN1A3 are recorded as A2. Under CS
103 condition, three biological replicates of HJG, HJGB1, HJGB2 and HJGB3, are denoted as B1;
104 three biological replicates of TN1, TN1B1, TN1B2 and TN1B3, are denoted as B2.

105 **RNA extraction, sequencing, assembly and annotation**

106 Total RNA was extracted with RNAprep Pure kit (Tiangen, Beijing, China) according to the
107 manufacturer's instructions. Nanodrop2000 (Shimadzu, Japan) was used to detect the

108 concentration and purity of the extracted RNA. Agarose gel electrophoresis was used to detect
109 the integrity of the RNA, and Agilent 2100 (Agilent, America) was used to determine the RIN
110 value. A single library requires 1 µg of RNA, with a concentration of ≥ 50 ng/µL, and
111 OD260/280 between 1.8 and 2.2. Magnetic beads (Invitrogen, America) with Oligo (dT) was
112 used to pair with the 3' poly A tail of eukaryotic mRNA, thus isolating mRNA from total RNA.
113 Subsequent, reverse synthesis of cDNA was performed. These libraries above were sequenced
114 using an Illumina NovaSeq 6000 sequencer (Illumina Inc., USA) and 150 bp paired-end reads
115 were generated. In order to ensure the accuracy of subsequent analysis, the original sequencing
116 data were filtered first to obtain clean data.

117 We used Trinity (Haas et al. 2013) to splice the transcript fragments to obtain transcripts, and
118 then used CD-HIT to cluster the transcript sequences to remove redundant sequences and get all
119 the unigene sequence sets for the subsequent analysis. Bowtie 2 (Salzberg et al. 2012) was used
120 to align the sequencing data to the reconstructed unigene sequence set, and the alignment file
121 was mainly used for subsequent unigene quantification and differential expression analysis. The
122 unigene sequences were compared with the NCBI non-redundant protein sequences (NR), Swiss-
123 Prot, TrEMBL, KEGG, GO, Pfam, and EuKaryotic Orthologous Groups (KOG) databases using
124 Basic Local Alignment Search Tool (BLAST). Finally, HMMER3 (Finn et al. 2011) was used to
125 align the amino acid sequence of unigene with the Pfam database to obtain the annotation
126 information of unigene.

127 **Enrichment analysis of DEGs**

128 The read counts and transcripts per million reads (TPM) were calculated using RSEM (Li et al.
129 2011) and bowtie2 (Salzberg et al. 2012). The DEGs were identified through the software
130 packages of Bioconductor 3.11-DESeq2 (Love et al. 2014). The screening threshold is false
131 discovery rate (FDR) < 0.05 , and \log_2 fold change (FC (condition 2/condition 1) for a gene) > 1
132 or \log_2 FC < -1 . The DEGs were classified, and GO and KEGG enrichment analysis were subsequently
133 performed.

134 **Weighted gene co-expression network analysis**

135 We followed these steps below for weighted gene co-expression network analysis (WGCNA): (i)
136 screening DEGs for WGCNA cluster analysis; (ii) calling the R package to cluster the DEGs; (iii)
137 calling ggplot2 in the R package to draw the clustering heat map and histogram of each module;
138 (iv) using the topGO to perform go enrichment analysis on each module; (v) calling Fisher-test
139 function in R for KEGG enrichment analysis; (vi) using Cytoscape3.8.0 (Su et al. 2014) to draw
140 network diagram.

141 **Validation of the chilling acclimation-related genes using RT-qPCR**

142 We selected 11 genes related to plant hormone signaling, fatty acid metabolism and plant-
143 pathogen interaction in GO and KEGG database, and 4 hub genes in WGCNA for validation.
144 The primers were designed using Primer3 (Table S1). Using *HIS* as the reference gene, RT-
145 qPCR was used to analyze the expression level of 15 genes in B1 and B2.

146 The identical RNA samples as the RNA-seq experiments were used for RT-qPCR analysis.
147 The detailed experimental method refers to Wu et al. (Wu et al. 2020). The relative gene
148 expression level was calculated by reference to the $2^{-\Delta\Delta C_t}$ method (Livak et al. 2001). All
149 expression analyses were performed in triplicates. The values represented arithmetic averages of
150 three replicates, and the data were expressed as a mean plus and minus standard deviation
151 (mean \pm SD).

152 **Statistical analysis**

153 CASAVA was used for base calling. Subsequently, we used SeqPrep for quality control of raw
154 sequencing data. Pearson correlation coefficient is used to measure the correlation between
155 samples. The package heatmap of R was used to prepare the correlation between samples and
156 DEGs expression pattern clustering. Data of RT-qPCR was analyzed using Excel 2007. The
157 figures were prepared using Origin 9.65.

158 **Results**

159 **Quality control and assembly of passion fruit transcriptome sequences**

160 To compare gene expression profiles of the two passion fruit cultivars under NT and CS,
161 transcriptome sequencing and analysis were performed. After decontamination and adaptor

162 removal, 533,935,574 raw reads were obtained from 12 samples, a total of 80.09 Gb clean reads
163 and 6.67 Gb per sample. The Q30 base percentage was 93.22% and GC content was 44.64%
164 (Table 1).

165 The clean reads were assembled into transcripts using the Trinity in paired-end method, and
166 211,874 transcript were obtained. The CD-HIT was then used to cluster the transcripts, which
167 yielded 47,353 unigenes with an average length of N50 of 2,368 bp, N90 of 450 bp, and an
168 average length of 1,211 bp. Afterwards, Bowtie2 was used to align the sequences of each sample
169 to the unigene sequence set, with an average alignment ratio of 77.89% (Table 2).

170 **Unigene function annotation**

171 The assembled unigenes were annotated to databases including the NR, Swiss-Prot, TrEMBL,
172 KEGG, GO, Pfam, and KOG, to which 97.92%, 70.40%, 97.82%, 33.97%, 36.16%, 61.43%, and
173 48.92% of unigenes were mapped, respectively. A total of 47,353 unigenes acquired annotation
174 information (Table 3). The number of annotated unigenes in NR and TrEMBL was the largest,
175 which were 46,369 and 46,323, respectively.

176 Using GO database, 17,123 unigenes were annotated and matched to three major categories:
177 biological process (BP), cellular component (CC) and molecular function (MF). Enriched BP
178 terms were mainly about “unigenes” (4,350), and “cellular process” (2,191). Enriched CC terms
179 mainly about “membrane part” (1,270), “cell part” (890). Enriched MF terms mainly about
180 “binding” (7,367), “catalytic activity” (5,715) (Fig. 1A).

181 Using KOG database, 23,164 unigenes were annotated. The unigenes were clustered into 25
182 categories. The unigenes were mainly about “signal transduction mechanisms” (2,439), and
183 “posttranslational modification, protein turnover, chaperones” (2,138) (Fig. 1B).

184 Using KEGG database, 16,086 unigenes were annotated. According to the functions, these
185 unigenes were enriched in 9 pathways. The enriched pathways were mainly about “metabolism”
186 (10,045), and “organismal systems” (4,505) (Fig. 1C).

187 **Comparative analysis of DEGs in two cultivars at two stages**

188 In order to gain insights on the adaptation of passion fruit to CS, the TPM method was used to

189 analyze the gene expression levels in the two stages (Fig. S1). The correlation coefficient
190 between the three biological replicates was 0.87 in HJGA, 0.98 in TN1A, 0.96 in HJGB, 0.99 in
191 TN1B, and the average correlation coefficient value was 0.95 (Fig. S2), indicating that the
192 reproducibility of this study was good and the experimental results were reliable.

193 The software package DESeq2 was used to perform differential expression analysis of
194 unigenes. There were 3,248 and 4,340 DEGs at two stages, respectively. After, analysis of the
195 DEGs for the two stages, we found that the number of DEGs between HJG and TN1 was
196 increased by 33.6% under CS condition (1,092), and 87.5% (955) were up-regulated (Fig. 2A).

197 Cluster analysis of gene expression can intuitively reflect the level of gene expression and
198 expression patterns in multiple samples. We used the DEGs to perform cluster analysis on A1 vs
199 A2 (Fig. 2B) and B1 vs B2 (Fig. 2C). The results showed that the difference between the three
200 biological replicates of each group was small, which again confirmed the rationality of sample
201 selection.

202 **GO and KEGG pathway enrichment analysis of DEGs**

203 There were 1,182 upregulated unigenes, and 2,066 downregulated unigenes at stage A; and there
204 were 2,137 upregulated unigenes and 2,203 downregulated unigenes at stage B.

205 GO enrichment analysis indicated that “metabolic process”(542), “oxidation-reduction process”
206 (156), “protein phosphorylation” (92), “carbohydrate metabolic process”(73), “organic substance
207 catabolic process” (40), and “catabolic process” (40), “extracellular region” (10), “apoplast” (8),
208 “cell wall” (8), “and external encapsulating structure” (8), “catalytic activity” (634), “transferase
209 activity” (228), “oxidoreductase activity” (167), “metal ion binding” (146), “cation binding”
210 (146), and “transition metal ion binding” were enriched at stage A (110) (Table S2). “oxidation-
211 reduction process” (187), “phosphate-containing compound metabolic process” (171),
212 “phosphorus metabolic process” (171), “macromolecule modification” (170), “cellular protein
213 modification process” (169), and “protein modification process” (169), “membrane” (213),
214 “intrinsic component of membrane” (99), and “integral component of membrane” (97), “catalytic
215 activity” (837), “transferase activity” (326), “cation binding” (202), “metal ion binding” (201),

216 “oxidoreductase activity” (198), “phosphotransferase activity”, and “alcohol group as acceptor”
217 (165) were enriched at B stage (Table S3).

218 The GO terms in A ($P > 0.05$) were compared to B ($P \leq 0.05$), and the unigenes were mainly
219 about “protein phosphorylation” (GO:0006468 , 61) “phosphorylation” (GO:0016310, 61),
220 “response to stimulus” (35), “lipid metabolic process” (19), “response to chemical” (13),
221 “membrane” (73), “intrinsic component of membrane” (29), “integral component of membrane”
222 (28) “catalytic activity”, “acting on a protein” (77), “transferase activity”, “transferring
223 phosphorus-containing groups” (70), “kinase activity” (67), “phosphotransferase activity”,
224 “alcohol group as acceptor” (67), and “protein kinase activity” (62) (Table S4).

225 The KEGG pathway enrichment analysis can reveal the main metabolic pathways and signal
226 transduction pathways in which the DEGs were involved, and the prevailing pathways were as
227 follows: “ribosome” (42), “carbon metabolism” (39), “biosynthesis of amino acids” (30), “starch
228 and sucrose metabolism” (21), “and cysteine and methionine metabolism” (20) at A stae; “plant
229 hormone signal transduction” (31), “plant-pathogen interaction” (27), “fatty acid metabolism”
230 (21), “cysteine and methionine metabolism” (20) (Fig. 3A). The KEGG pathway in A($P > 0.05$)
231 werecompared to B ($P \leq 0.05$), and the unigenes were mainly about“plant-pathogen interaction”
232 (17), “plant hormone signal transduction” (14), and “fatty acid metabolism” (8) (Fig. 3B).

233 WGCNA analysis

234 After background correction and normalization of the unigenes expression data, we filtered out
235 the abnormal and minor change unigenes. Fianlly, and obtained 12,471 highly expressed
236 unigenes. In this study, when the soft threshold was 16 (Fig. S3), the gene topology matrix
237 expression network was closest to the scale-free distribution. A gene cluster tree was constructed
238 based on the correlation between genes, and each branch corresponded to a cluster of gene sets
239 with highly correlated expression levels (Fig. S4a).

240 According to the standard of mixed dynamic shear, the gene modules were classified and the
241 eigenvector of each module was calculated. The modules close to each other were merged, and 8
242 co-expression modules were obtained (Fig. S4b). Each module used different colors to represent

243 the clustered genes. The turquoise module had the most clustered genes (4,171), the red module
244 contained the fewest (81), and the grey module contained the unigenes that couldn't be included
245 in any module.

246 The DEGs were used to draw the heat map of each module in the 4 sample groups. The brown
247 and yellow modules showed less changes in differential unigenes between the early and late HJG,
248 but showed larger changes in differential unigenes between early and late TN1 (Fig.4), which is
249 consistent with the chilling resistance feature of TN1. Therefore, we selected the unigenes of
250 these two modules for in-depth GO and KEGG pathway analysis.

251 In the brown module, the GO terms significantly enriched in “cellular macromolecule
252 metabolic process”, “phosphate-containing compound metabolic process”, “phosphorus
253 metabolic process”, “protein phosphorylation”, “stimulus” “transferase complex”, “riboflavin
254 synthase complex”, “photosystem I reaction center”, “photosystem I” “binding”, “metal ion
255 binding”, “cation binding”, “phosphotransferase activity”, “alcohol group as acceptor”, “kinase
256 activity” (Table S5). In the KEGG pathway analysis, the prevailing pathways were “plant
257 hormone signal transduction”, “MAPK signaling pathway”, “starch and sucrose metabolism”
258 (Fig. 5A).

259 In the yellow module, the GO terms significantly enriched in “cellular process”,
260 “macromolecule modification”, “phosphorus metabolic process”, “cellular protein modification
261 process”, “protein modification process”, “cell periphery”, “photosystem”, “photosynthetic
262 membrane”, “thylakoid”, “extracellular region” “3-deoxy-7-phosphoheptulonate synthase
263 activity”, “alkylbase DNA N-glycosylase activity”, “DNA-3-methyladenine glycosylase
264 activity”, “DNA N-glycosylase activity”, and “method adenosyltransferase activity” (Table S6).
265 The significantly enriched pathways included “biosynthesis of amino acids”, “plant hormone
266 signal transduction”, “ABC transporters”, “starch and sucrose metabolism”, “folate biosynthesis”
267 and “other pathways” that might be related to CS (Fig. 5B).

268 We used Cytoscape to prepare network diagram in the brown and yellow module, and got 19
269 hub unigenes which mainly related to “MAPK signaling pathway”, “plant hormone signal

270 transduction”, “starch and sucrose metabolism”, “fatty acid biosynthesis” and “photosynthesis in
271 the brown module” (Fig. 6A). In the yellow module, we obtained 13 hub unigenes which mainly
272 related to “plant hormone signal transduction”, “MAPK signaling pathway”, “starch and sucrose
273 metabolism” and “fatty acid degradation” (Fig. 6B).

274 **Validation of gene expression changes during chilling acclimation**

275 We used the RT-qPCR method to validate the expression level of 15 unigenes. The results
276 showed that the RT-qPCR expression patterns of the 15 unigenes were consistent with RNA-seq
277 analysis (Fig. 7, Table S7). RT-qPCR analysis showed that the 9 fold-change unigenes were ≥ 2 or
278 ≤ 0.5 . Comparison with B1 and B2, TPM values of 12 unigenes were ≥ 2 or ≤ 0.5 . The results
279 showed that 9 out 12 DEGs could be validated using RT-qPCR, and DEGs analysis were highly
280 reliable.

281 **Discussions**

282 Low temperature is one of the main abiotic stresses that plants are vulnerable to during their life
283 cycle, and the response of plants to low temperature stress is a multi-factor synergistic process
284 involving complex physiological and gene expression regulatory networks. With the
285 development of molecular biology technology, researchers have cloned many key genes of low
286 temperature signal pathway *Arabidopsis thaliana* (Wang et al. 2019; Ding et al. 2018; Ye et al.
287 2019) and rice (Ma et al. 2015; Zhang et al. 2017A). Passion fruit is a tropical and subtropical
288 fruit tree and it is vulnerable to low temperature in winter which causes great economic losses.
289 However, there are fewer studies on cold stress in passion fruit. In this study, the passion fruit
290 variety of ‘Tainong 1’ was identified, which has the characteristics of cold-tolerance.

291 Although the two cDNA libraries were constructed for transcriptome sequencing in passion
292 fruit under CS condition (Liu et al. 2017A), we still know little about the cold tolerance of
293 passion fruit. To reveal the molecular mechanisms of chilling acclimation of passion fruits
294 under CS, RNA-seq and analysis were performed. Using database function annotation, we
295 obtained 47,353 unigenes. Based on RNA-seq data, the number of down-regulated DEGs did
296 not change much at two stages, but the number of up-regulated differential unigenes were 955,

297 indicating that the up-regulation of DEGs might be related to the chilling acclimation.

298 Protein phosphorylation is also a type of post-translational regulation during the cold
299 acclimation of plant. Under cold condition, CRPK1 is activated and phosphorylates 14-3-3 λ , and
300 the phosphorylated 14-3-3 λ enters nucleus from the cytoplasm and degrades CBFs via direct
301 interaction in *Arabidopsis* (Liu et al. 2017B). Transcriptome sequencing revealed that 61 DEGs
302 of protein phosphorylation and phosphorylation were significantly upregulated or downregulated
303 in the two stages, respectively (Table S4). Furthermore, the unigenes mainly related to calcium-
304 dependent protein kinase, serine/threonine-protein kinase, and CBL-interacting serine/threonine-
305 protein kinase. In rice, calcium-dependent protein kinase gene OsCPK17 (Almadanim et al.
306 2018), OsCDPK7 (Saijo et al. 2000) and OsCPK24 (Liu et al. 2018B) all respond to low
307 temperature. In previous study, serine/threonine protein kinase responses to cold stress (Soto et al.
308 2002). These results indicated that protein phosphorylation could play an important role in cold
309 acclimation of passion fruit.

310 Mitogen-activated protein kinase (MAPK) plays an important role in signal transduction, and
311 is also essential for regulating the cold response of plants. Under low temperature, the
312 phosphorylation levels of MPK3, MPK4 and MPK6 were significantly increased (Zhao et al.
313 2017B); moreover, MPK3 and MPK6 could interact with ICE1 to participate in low-temperature
314 response (Li et al.). Zhang et al. found that the phosphorylated OsICE1 could promote *OsTPP1*
315 transcription and induce the production of large amounts of trehalose, thereby improving the cold
316 resistance of rice (Zhang et al. 2017B). Using WGCNA analysis, we found that MAPK signaling
317 pathway significantly enriched in the brown module, which contained 7 DEGs (Figure 5A).
318 Moreover, the functional annotation of TRINITY_DN36339_c2_g1_i5 was mitogen activated
319 protein kinase kinase kinase 3. In rice, OsMKK6 and OsMPK3 constitute a moderately low-
320 temperature signalling pathway and regulate cold stress tolerance (Xie et al. 2012). MKK2
321 induces the expression of COR genes to enhance the freezing tolerance of *Arabidopsis* (Teige et
322 al. 2004).

323 In plants, hormones and cold signaling pathways are coordinated to better adapt to cold stress.

324 ABA is used as an important signal molecule and the most important stress signal in hormones,
325 and it can mediate the signal transduction pathway to cold stress and increase the tolerance of
326 cold stress (Yuan et al. 2018B). Auxin acts as a trigger in plant growth and development. In rice,
327 ROC1 can regulate *CBF1*, and auxin can affect ROC1 levels (Dou et al. 2016). In addition, BR,
328 GA, JA, ethylene, CK, and melatonin play important regulatory roles in the ICE–CBF–COR
329 pathway (Wang et al. 2017). In CS condition, we found 31 unigenes about plant hormone signal
330 transduction (Figure 3A). In WGCNA analysis, the pathway of plant hormone signal
331 transduction was enriched in brown and yellow modules. These unigenes were annotated about
332 aux, JA, ABA, and BR.

333 Plants use fatty acid dehydrogenase to regulate the increase of fatty acid unsaturation to
334 improve the cold resistance (Upchurch 2008; He et al. 2015). The change of malondialdehyde
335 content caused by lipid peroxidation is negatively correlated with plant cold resistance (Kim et al.
336 2011). In this study, the unigenes related to fatty acid metabolism and lipid metabolic process
337 were identified (Figure 3A, Figure 6B). Among them, 16 unigenes were annotated as delta(12)-
338 fatty-acid desaturase (*FAD2*). In rice, *OsFAD2* is involved in fatty acid desaturation and
339 maintenance of the membrane lipids balance in cells, and could improve the low temperature
340 tolerance (Shi et al. 2012). Similarly, *FAD2* could improve the salt tolerance during seed
341 germination and early seedling growth (Zhang et al. 2012), but *FAD8* was strongly inducible by
342 low temperature in *Arabidopsis thaliana* (Gibson et al. 1994). The results indicated that *FAD2*
343 could improve the CS of passion fruit.

344 In the process of cold acclimation in plants, the hydrolysis of starch is intensified and the
345 content of soluble sugar increases. As a result, the freezing point of cell fluid is lowered and the
346 excessive dehydration of cells is reduced (Krasensky j 2012; Yue et al. 2015). The analysis of
347 pathway enriched by KEEG and WGCNA revealed starch and sucrose metabolism related to
348 cold stress was enriched at stage B. Three DEGs were obtained at stage B compare to stage A,
349 and these unigenes were annotated as beta-glucosidase and glucan endo-1,3-beta-glucosidase 3-
350 like genes.

351 **Conclusions**

352 In this study, we performed a comprehensive comparative transcriptome analysis firstly
353 between two passion fruit cultivars, to identify the gene expression level and analyze molecular
354 mechanism of chilling acclimation. This work showed that the unigenes of protein
355 phosphorylation, MAPK signaling, plant hormones and fatty acid metabolism play important
356 roles in the chilling tolerance between the two passion fruit cultivars. Furthermore, 32 hub
357 unigenes were assigned to modules and played a regulatory role in the chilling acclimation of
358 passion fruit. In all, these findings provide a deepened understanding of the molecular
359 mechanism of cold stress and could facilitate the genetic improvement of chilling tolerance in
360 passion fruit.

361 **Acknowledgments**

362 The authors thank to Dr. Yinghua Pan for help providing data analysis suggestions.

363 **References**

- 364 **Almadanim MC, Gonçalves NM, Rosa M, Alexandre BM, Cordeiro AM, Rodrigues M, Saibo N, Soares**
365 **CM, Romão CV, Oliveira MM, Abreu IA. 2018.** The rice cold-responsive calcium-dependent protein
366 kinase OsCPK17 is regulated by alternative splicing and post-translational modifications. *Biochim*
367 *Biophys Acta Mol Cell Res* **1865**: 231-246.
- 368 **Carpaneto A, Ivashikina N, Levchenko V, Krol E, Jeworutzki E, Zhu J, Hedrich H. 2007.** Cold
369 transiently activates calcium-permeable channels in Arabidopsis mesophyll cells. *Plant Physiol* **143**: 487-
370 494.
- 371 **Catalá R, Medina J, Salinas J. 2011.** Integration of low temperature and light signaling during cold
372 acclimation response in Arabidopsis. *Proc Natl Acad Sci U S A* **108**: 16475-16480.
- 373 **Chinnusamy V, Ohta M, Kanrar S, Lee BH, Hong X, Agarwal M, Zhu JK. 2003.** ICE1: a regulator of
374 cold-induced transcriptome and freezing tolerance in Arabidopsis. *Genes Dev* **17**: 1034-1054.
- 375 **Ding Y, Jia Y, Shi Y, Zhang X, Song C, Gong Z, Yang S. 2018.** OST1-mediated BTF3L phosphorylation
376 positively regulates CBFs during plant cold responses. *EMBO J* **37**: e98228.
- 377 **Doherty CJ, Van buskirk HA, Myers SJ, Thomashow MF. 2009.** Roles for arabidopsis camta transcription
378 factors in cold-regulated gene expression and freezing tolerance. *Plant Cell* **21**: 972-984.
- 379 **Dou M, Cheng S, Zhao B, Xuan Y, Shao M. 2016.** The indeterminate domain protein ROC1 regulates
380 chilling tolerance via activation of DREB1B/CBF1 in rice. *Int J Mol Sci* **17**: 233.
- 381 **Finn RD, Clements J, Eddy SR. 2011.** HMMER web server: interactive sequence similarity searching.
382 *Nucleic Acids Res* **39**: W29-W37.
- 383 **Gibson S, Arondel V, Iba K, Somerville C. 1994.** Cloning of a temperature-regulated gene encoding a
384 chloroplast ω -3 desaturase from Arabidopsis thaliana. *Plant Physiol* **106**: 1615-1621.
- 385 **Guo X, Liu D, Chong K. 2018.** Cold signaling in plants: Insights into mechanisms and regulation. *J Integr*

- 386 Plant Biol **60**: 745-756.
- 387 **Haas BJ, Papanicolaou A, Yassour M, Grabherr M, Blood PD, Bowden J, Couger MB, Eccles D, Li B,**
388 **Lieber M, Macmanes MD, Ott M, Orvis J, Pochet N, Strozzi F, Weeks N, Westerman R, William T,**
389 **Dewey CN, Henschel R, Leduc RD, Friedman N, Regev A. 2013.** De novo transcript sequence
390 Reconstruction from RNA-seq using the Trinity platform for reference Generation and analysis. Nat
391 Protoc **8**: 1494-1512.
- 392 **Hara M, Terashima S, Fukaya T, Kuboi T. 2003.** Enhancement of cold tolerance and inhibition of lipid
393 peroxidation by citrus dehydrin in transgenic tobacco. Planta **217**: 290-298.
- 394 **He J, Yang Z, Hu B, Ji X, Wei Y, Lin L, Zhang Q. 2015.** Correlation of polyunsaturated fatty acids with the
395 cold adaptation of *Rhodotorula glutinis*. Yeast **32**: 683-690.
- 396 **Hendrickson L, Vlcková A, Selstam E, Huner N, Oquist G, Hurry V. 2006.** Cold acclimation of the
397 *Arabidopsis* *dgd1* mutant results in recovery from photosystem I-limited photosynthesis. FEBS Lett **580**:
398 4959-4968.
- 399 **Kim SI, Tai TH. 2011.** Evaluation of seedling cold tolerance in rice cultivars: a comparison of visual ratings
400 and quantitative indicators of physiological changes. Euphytica **178**: 437-447.
- 401 **Kim SH, Kim HS, Bahk S, An J, Yoo Y, Jy K, Chung WS. 2017.** Phosphorylation of the transcriptional
402 repressor MYB15 by mitogen-activated protein kinase 6 is required for freezing tolerance in *Arabidopsis*.
403 Nucleic Acids Res **45**: 6613-6627.
- 404 **Krasensky j JC. 2012.** Drought, salt, and temperature stress-induced metabolic rearrangements and regulatory
405 networks. J Exp Bot **63**: 1593-1608.
- 406 **Krishnan N, Dickman MB, Becker DF. 2008.** Proline modulates the intracellular redox environment and
407 protects mammalian cells against oxidative stress. Free Radic Biol Med **44**: 671-681.
- 408 **Li H, Ding YL, Shi YT, Zhang XY, Zhang SQ, Gong ZZ, Yang SH. 2017.** MPK3- and MPK6-mediated ICE1
409 phosphorylation negatively regulates ICE1 stability and freezing tolerance in *Arabidopsis*. Dev Cell **43**:
410 630-642.
- 411 **Li B, Dewey CN. 2011.** RSEM: accurate transcript quantification from RNA-Seq data with or without a
412 reference genome. BMC Bioinformatics **12**: 323.
- 413 **Liu Q, Kasuga M, Sakuma Y, Abe H, Miura S, Yamaguchi-shinozaki K, Shinozaki K. 1998.** Two
414 transcription factors, DREB1 and DREB2, with an EREBP/AP2 DNA binding domain separate two
415 cellular signal transduction pathways in drought- and low-temperature-responsive gene expression,
416 respectively, in *Arabidopsis*. Plant Cell **10**: 1391-1406.
- 417 **Liu S, Li AD, Chen CH, Cao GJ, Zhang LM, Guo CY, Xu M. 2017A.** DE NOVO transcriptome sequencing
418 in *passiflora edulis* SIMS to identify genes and signaling pathways involved in cold tolerance. Forests **8**:
419 435.
- 420 **Liu Z, Jia Y, Ding Y, Shi Y, Li Z, Guo Y, Gong Z, Yang S. 2017B.** Plasma membrane CRPK1-mediated
421 phosphorylation of 14-3-3 proteins induces their nuclear import to fine-tune CBF signaling during cold
422 response. Mol Cell **66**: 117-128.
- 423 **Liu J, Shi Y, Yang S. 2018A.** Insights into the regulation of C-repeat binding factors in plant cold signaling. J
424 Integr Plant Biol **60**: 780-795.
- 425 **Liu Y, Xu C, Zhu Y, Zhang L, Chen T, Zhou F, Chen H, Lin Y. 2018B.** The calcium-dependent kinase
426 OsCPK24 functions in cold stress responses in rice. J Integr Plant Biol **60**: 173-188.

- 427 **Liu X, Fu L, Qin P, Sun Y, Liu J, Wang X. 2019.** Overexpression of the wheat trehalose 6-phosphate
428 synthase 11 gene enhances cold tolerance in *Arabidopsis thaliana*. *Gene* **710**: 210-217.
- 429 **Livak KJ, Schmittgen TD. 2001.** Analysis of relative gene expression data using real-time quantitative PCR
430 and the 2⁻($\Delta\Delta C_T$) Method. *Methods* **25**: 402-408.
- 431 **Love MI, Huber W, Anders S. 2014.** Moderated estimation of fold change and dispersion for RNA-seq data
432 with DESeq2. *Genome Biol* **15**: 550.
- 433 **Ma Y, Dai X, Xu Y, Luo W, Zheng X, Zeng D, Pan Y, Lin X, Liu H, Zhang D, Xiao J, Guo X, Xu S, Niu
434 Y, Jin J, Zhang H, Xu X, Li L, Wang W, Qian Q, Ge S, Chong K. 2015.** COLD1 confers chilling
435 tolerance in rice. *Cell* **160**: 1209-1221.
- 436 **Mann m JO. 2003.** Proteomic analysis of post-translational modifications. *Nat Biotechnol* **21**: 255-261.
- 437 **Saijo Y, Hata S, Kyojuka J, Shimamoto K, Izui K. 2000.** Over-expression of a single Ca²⁺-dependent
438 protein kinase confers both cold and salt/drought tolerance on rice plants. *Plant J* **23**: 319-327.
- 439 **Salzberg SL, Langmead B. 2012.** AST gapped-read alignment with bowtie 2. *Nat Methods* **9**: 357-359.
- 440 **Seong es BS, Cho hs CD. 2007.** Induction of enhanced tolerance to cold stress and disease by overexpression
441 of the pepper CAPIF1 gene in tomato. *Physiol Plant* **129**: 555-566.
- 442 **Shi J, Cao Y, Fan X, Li M, Wang Y, Ming F. 2012.** A rice microsomal delta-12 fatty acid desaturase can
443 enhance resistance to cold stress in yeast and *Oryza sativa*. *Mol Breeding* **29**: 743-757.
- 444 **Shi Y, Ding Y, Yang S. 2018.** Molecular regulation of CBF signaling in cold acclimation. *Trends Plant Sci* **23**:
445 623-637.
- 446 **Soto T, Beltrán FF, Paredes V, Madrid M, Millar JB, Vicente-soler J, Cansado J, Gacto M. 2002.** Cold
447 induces stress-activated protein kinase-mediated response in the fission yeast *Schizosaccharomyces*
448 *pombe*. *Eur J Biochem* **269**: 5056-5065.
- 449 **Stockinger EJ, Gilmour SJ, Thomashow MF. 1997.** *Arabidopsis thaliana* CBF1 encodes an AP2 domain-
450 containing transcriptional activator that binds to the C-repeat/DRE, a cis-acting DNA regulatory element
451 that stimulates transcription in response to low temperature and water deficit. *Proc Natl Acad Sci U S A*
452 **94**: 1035-1040.
- 453 **Su G, Morris JH, Demchak B, Bader GD. 2014.** Biological network exploration with Cytoscape 3. *Curr*
454 *Protoc Bioinformatics* **8**: 8.13.1–8.1.
- 455 **Teige M, Scheikl E, Eulgem T, Dóczi R, Ichimura K, Shinozaki K, Dangl JL, Hirt H. 2004.** The MKK2
456 pathway mediates cold and salt stress signaling in *Arabidopsis*. *Mol Cell* **15**: 141-152.
- 457 **Upchurch RG. 2008.** Fatty acid unsaturation, mobilization, and regulation in the response of plants to stress.
458 *Biotechnol Lett* **30**: 967-977.
- 459 **Vogel JT, Zarka DG, Van buskirk HA, Fowler SG, Thomashow MF. 2005.** Roles of the CBF2 and ZAT12
460 transcription factors in configuring the low temperature transcriptome of *Arabidopsis*. *Plant J* **41**: 195-211.
- 461 **Wang DZ, Jin YN, Ding XH, Wang WJ, Zhai SS, Bai LP, Guo ZF. 2017.** Gene regulation and signal
462 transduction in the ICE-CBF-COR signaling pathway during cold stress in plants. *Biochemistry (Mosc)*
463 **82**: 1103-1117.
- 464 **Wang H, Tang J, Liu J, Hu J, Liu J, Chen Y, Cai Z, Wang X. 2018.** Abscisic acid signaling inhibits
465 brassinosteroid signaling through dampening the dephosphorylation of BIN2 by ABI1 and ABI2. *Mol*
466 *Plant* **11**: 315-325.
- 467 **Wang X, Ding Y, Li Z, Shi Y, Wang J, Hua J, Gong Z, Zhou JM, Yang S. 2019.** PUB25 and PUB26

- 468 promote plant freezing tolerance by degrading the cold signaling negative regulator MYB15. *Dev Cell* **51**:
469 222-235.
- 470 **Webb MS, Uemura M, Steponkus PL. 1994.** A comparison of freezing injury in oat and rye: two cereals at
471 the extremes of freezing tolerance. *Plant Physiol* **104**: 467-478.
- 472 **Wu J, Zhang Y, Yin L, Qu J, Lu J. 2014.** Linkage of cold acclimation and disease resistance through plant-
473 pathogen interaction pathway in *Vitis amurensis* grapevine. *Funct Integr Genomics* **14**: 741-755.
- 474 **Wu Y, Tian Q, Huang W, Liu J, Xia X, Yang X, Mou H. 2020.** Identification and evaluation of reference
475 genes for quantitative real-time PCR analysis in *Passiflora edulis* under stem rot condition. *Mol Biol Rep*
476 **47**: 2951-2962.
- 477 **Xie G, Kato H, Imai R. 2012.** Biochemical identification of the OsMKK6-OsMPK3 signalling pathway for
478 chilling stress tolerance in rice. *Biochem J* **443**: 95-102.
- 479 **Yadav SK. 2010.** Cold stress tolerance mechanisms in plants. *Agron Sustain Dev* **30**: 605-620.
- 480 **Yamori W, Hikosaka K, Way DA. 2014.** Temperature response of photosynthesis in C3, C4, and CAM
481 plants: temperature acclimation and temperature adaptation. *Photosynth Res* **119**: 101-117.
- 482 **Ye K, Li H, Ding Y, Shi Y, Song C, Gong Z, Yang S. 2019.** BRASSINOSTEROID-INSENSITIVE2
483 negatively regulates the stability of transcription factor ICE1 in response to cold stress in *Arabidopsis*.
484 *Plant Cell* **31**: 2682-2696.
- 485 **Yuan P, Du L, Poovaiah BW. 2018A.** Ca²⁺/Calmodulin-dependent AtSR1/CAMTA3 plays critical roles in
486 balancing plant growth and immunity. *Int J Mol Sci* **19**: E1764.
- 487 **Yuan P, Yang T, Poovaiah BW. 2018B.** Calcium signaling-mediated plant response to cold stress. *Int J Mol*
488 *Sci* **19**: E3896.
- 489 **Yue C, Cao HL, Wang L, Zhou YH, Huang YT, Hao XY, Ye W, Wang B, Yang YJ, Wang XC. 2015.**
490 Effects of cold acclimation on sugar metabolism and sugar-related gene expression in tea plant during the
491 winter season. *Plant Mol Biol* **88**: 591-608.
- 492 **Zhang J, Liu H, Sun J, Li B, Zhu Q, Chen S, Zhang H. 2012.** *Arabidopsis* fatty acid desaturase FAD2 is
493 required for salt tolerance during seed germination and early seedling growth. *PLoS One* **7**: e30355.
- 494 **Zhang Z, Li J, Pan Y, Li J, Zhou L, Shi H, Zeng Y, Guo H, Yang S, Zheng W, Yu J, Sun X, Li G, Ding Y,
495 Ma L, Shen S, Dai L, Zhang H, Yang S, Guo Y, Li Z. 2017A.** Natural variation in CTB4a enhances
496 rice adaptation to cold habitats. *Nat Commun* **8**: 14788.
- 497 **Zhang Z, Li J, Li F, Liu H, Yang W, Chong K, Xu Y. 2017B.** OsMAPK3 phosphorylates
498 OsbHLH002/OsICE1 and inhibits its ubiquitination to activate OsTPP1 and enhances rice chilling
499 tolerance. *Dev Cell* **43**: 731-745.
- 500 **Zhang F, Lu K, Gu Y, Zhang L, Li W, Li Z. 2020.** Effects of low-temperature stress and brassinolide
501 application on the photosynthesis and leaf structure of tung tree seedlings. *Front Plant Sci* **10**: 1767.
- 502 **Zhao C, Wang P, Si T, Hsu CC, Wang L, Zayed O, Yu Z, Zhu Y, Dong J, Tao W, Zhu JK. 2017A.** MAP
503 kinase cascades regulate the cold response by modulating ICE1 protein stability. *Dev Cell* **43**: 618-629.
- 504 **Zhao C, Wang P, Si T, Hsu CC, Wang L, Zayed O, Yu Z, Zhu Y, Dong J, Tao W, Zhu JK. 2017B.** Map
505 kinase cascades regulate the cold response by modulating ICE1 protein stability. *Dev Cell* **43**: 618-629.

Table 1 (on next page)

Statistical results of transcriptome sequencing

1

2

Table 1 Statistical results of transcriptome sequencing

Sample	Reads number	Total base (bp)	Q30 (%)	GC content (%)
HJGA1	46599672	6989950800	93.02	45.36
HJGA2	44522400	6678360000	93.08	44.49
HJGA3	46642622	6996393300	93.23	45.31
TN1A1	47166760	7075014000	93.18	45.23
TN1A2	43505726	6525858900	93.31	44.33
TN1A3	45058566	6758784900	93.16	43.83
HJGB1	44758052	6713707800	93.34	43.83
HJGB2	43843522	6576528300	93.43	44.70
HJGB3	39087142	5863071300	93.14	43.37
TN1B1	49306634	7395995100	93.31	45.51
TN1B2	44267228	6640084200	93.17	44.87
TN1B3	39177250	5876587500	93.27	44.89

3

Table 2 (on next page)

Sequencing data mapped to unigene set

1

2

Table 2 Sequencing data mapped to unigene set

Sample	Pair reads	Aligned concordantly 0 times	Aligned concordantly exactly 1 time	Aligned concordantly >1 times	Total alignment ratio (%)
HJGA1	23299836	6183910	15486803	1629123	83.19
HJGA2	22261200	6461646	14313504	1486050	81.73
HJGA3	23321311	7002139	14768806	1550366	81.04
TN1A1	23583380	8597970	13025983	1959427	75.69
TN1A2	21752863	7919003	11974898	1858962	75.79
TN1A3	22529283	7817813	12764435	1947035	77.11
HJGB1	22379026	6946292	14131411	1301323	78.91
HJGB2	21921761	6859052	13821399	1241310	78.45
HJGB3	19543571	5267390	12862365	1413816	81.72
TN1B1	24653317	9000336	13737412	1915569	74.21
TN1B2	22133614	8908390	11548761	1676463	70.83
TN1B3	19588625	6676080	11320050	1592495	75.95

3

Table 3 (on next page)

Unigenes were annotated to 7 databases

1

2

Table 3 Unigenes were annotated to 7 databases

Database	Annotated number	Annotated ratio (%)
GO	17123	36.16
KEGG	16086	33.97
KOG	23164	48.92
NR	46369	97.92
Pfam	29091	61.43
Swiss-Prot	33337	70.40
TrEMBL	46323	97.82
Total	47353	100

3

Figure 1

Annotation of passion fruit transcriptome

(A) GO function classification diagram of unigenes. The x-axis indicates the secondary classification terms of GO; the y-axis indicates the number of unigenes in this secondary classification out of the total annotated unigenes. (B) KOG functional annotation distribution of unigenes. The x-axis indicates the number of unigenes; the y-axis indicates the name of 25 groups. (C) KEGG classification of unigenes. The x-axis indicates the number of unigenes in the pathway; the y-axis indicates KEGG pathways.

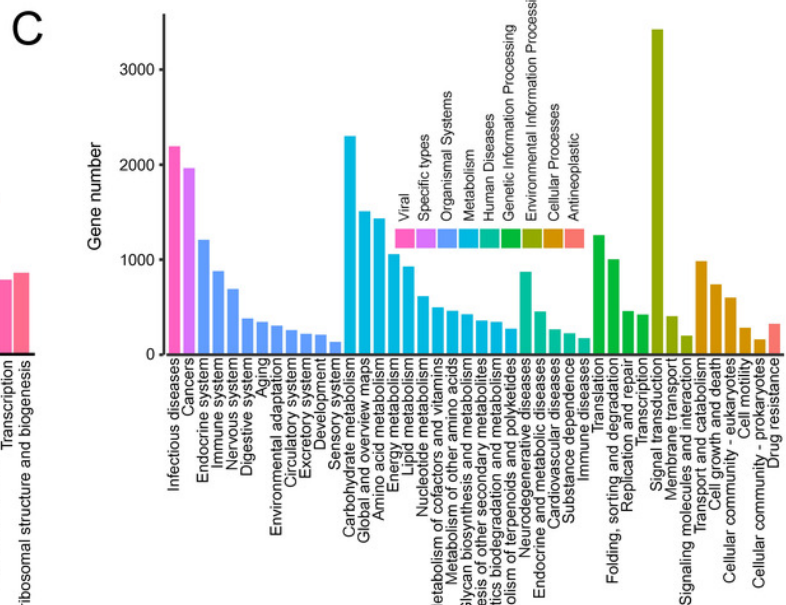
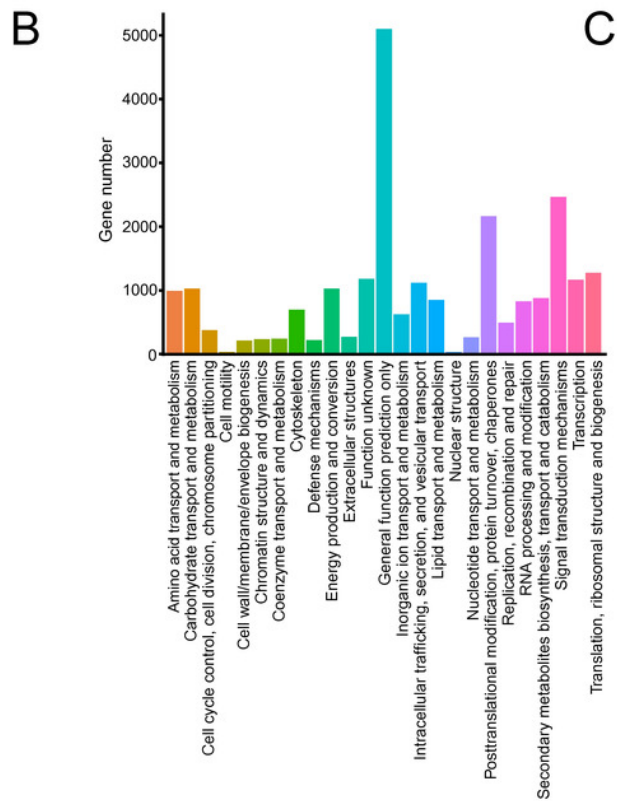
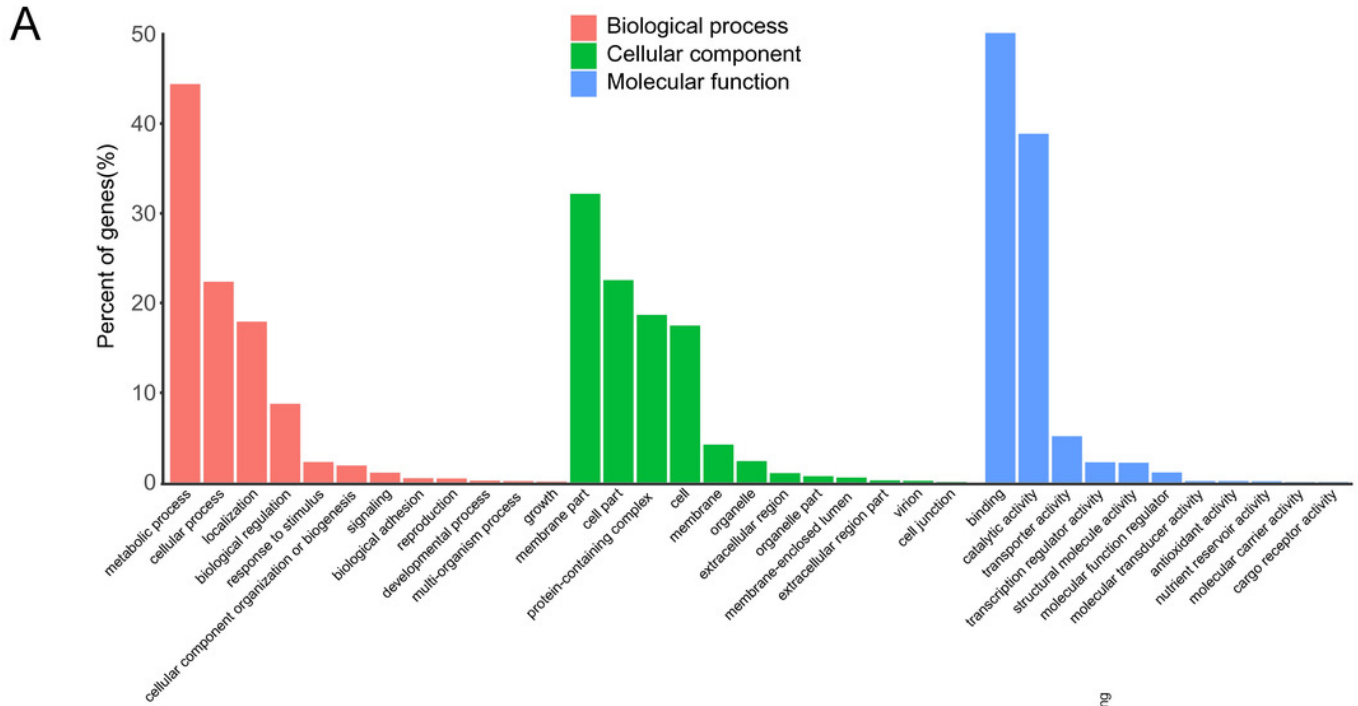


Figure 2

Analysis of DEGs at two stages.

(A) DEGs identified between HJG and TN1. (B) A1 vs A2; (C) B1 vs B2. Red indicates that the gene is highly expressed in the sample; blue indicates lower expression, and the number label under the color bar at the upper left is the specific trend of the change of expression. The left is a dendrogram of gene clustering, and below is the name of the samples. Figure 3 **KEGG pathway enrichment of DEGs.** (A) A1 vs A2. (B) B1 vs B2. The left is the name of pathways, and below is the enrichment factor. The size of the dots indicate the number of genes in this pathway, and the color of the dots corresponds to different $-\log_{10}(\text{correct } p \text{ value})$ ranges.

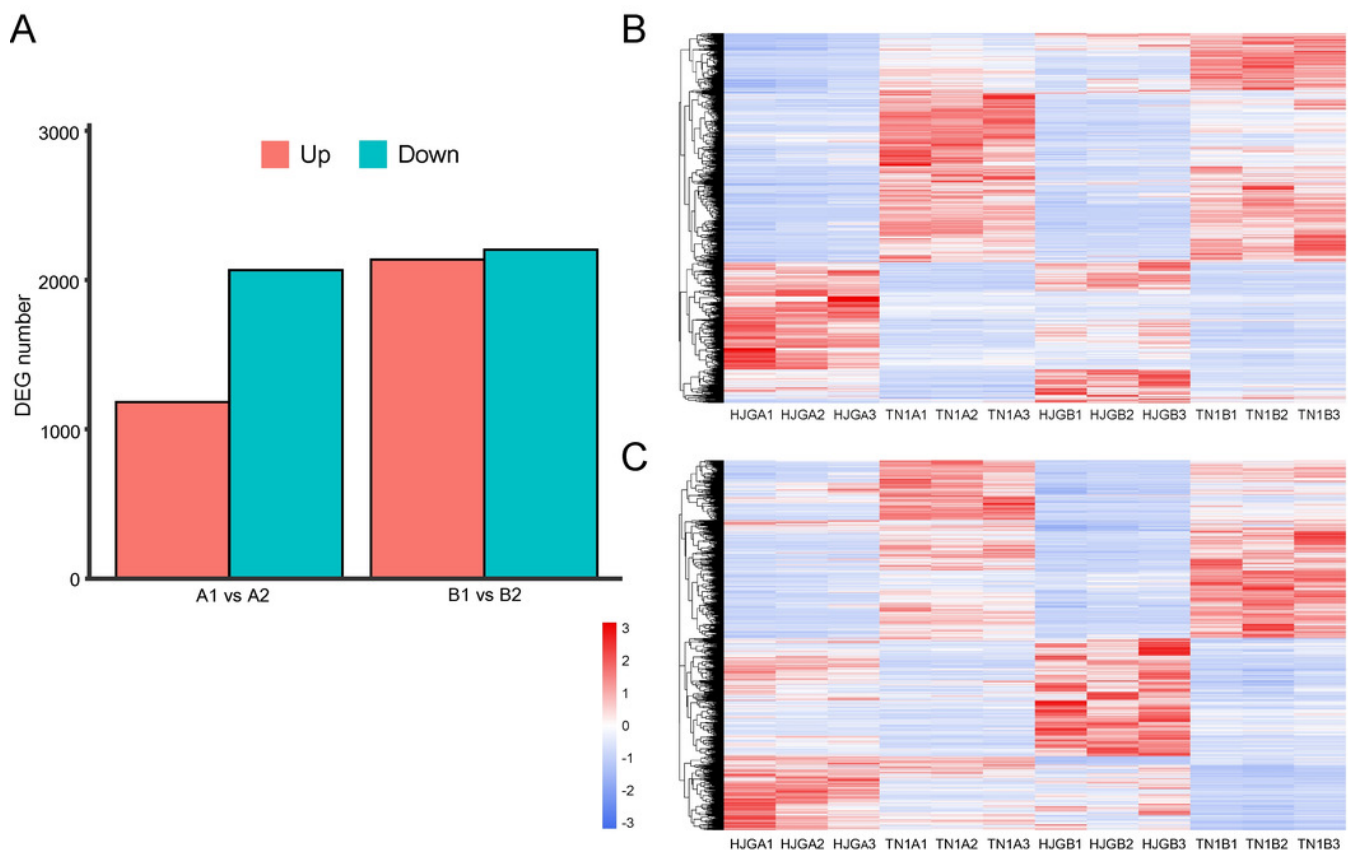


Figure 3

KEGG pathway enrichment of DEGs.

(A) A1 vs A2. (B) B1 vs B2. The left is the name of pathways, and below is the enrichment factor. The size of the dots indicate the number of genes in this pathway, and the color of the dots corresponds to different $-\log_{10}(\text{correct p value})$ ranges.

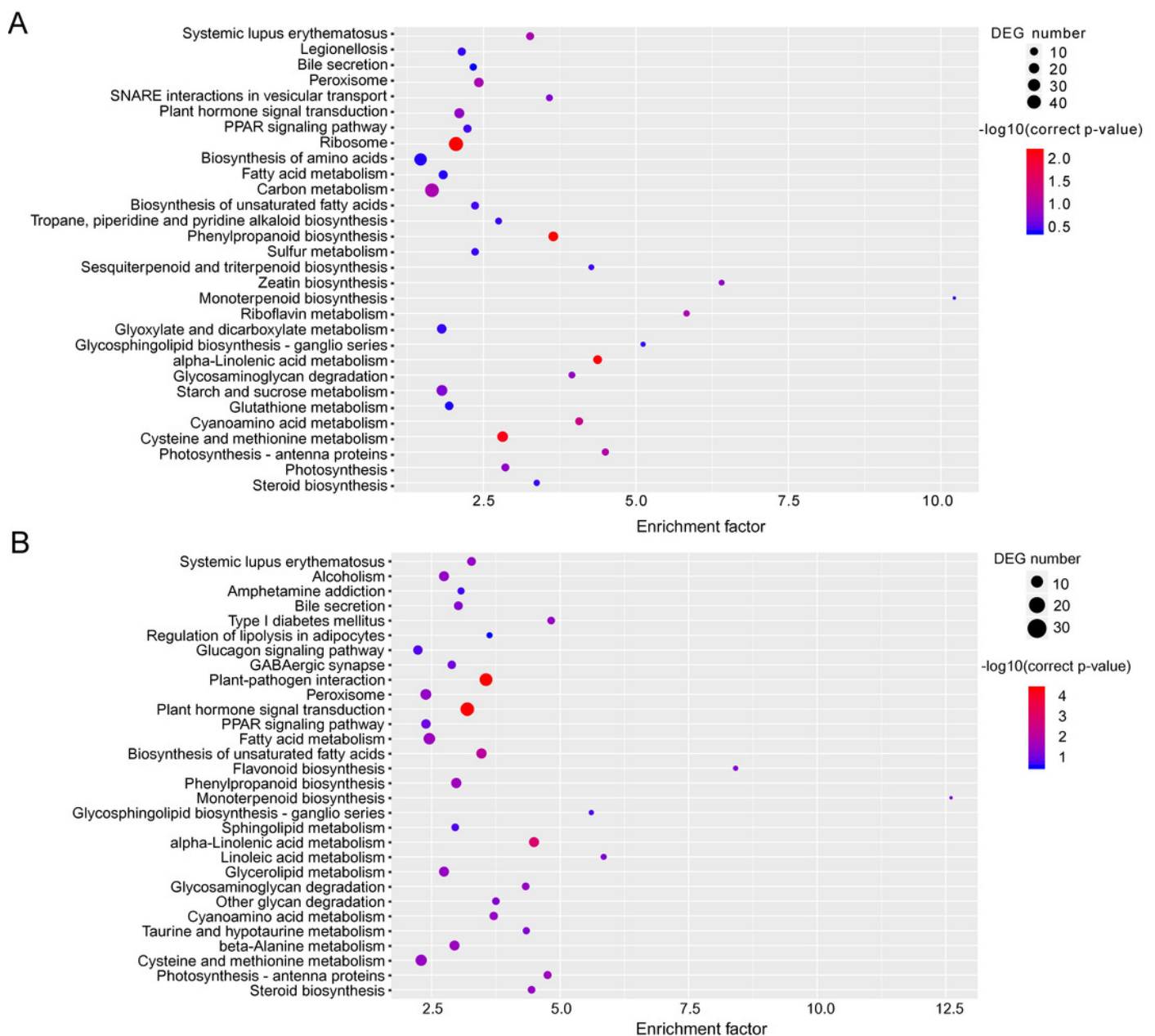


Figure 4

The heat map of DEGs at two stages.

(A) A1 vs A2. (B) B1 vs B2. The below is the name of the samples. Red indicates that the gene is highly expressed in the sample; blue indicates lower expression, and the number label under the color bar at the upper left is the specific trend of the change of expression.

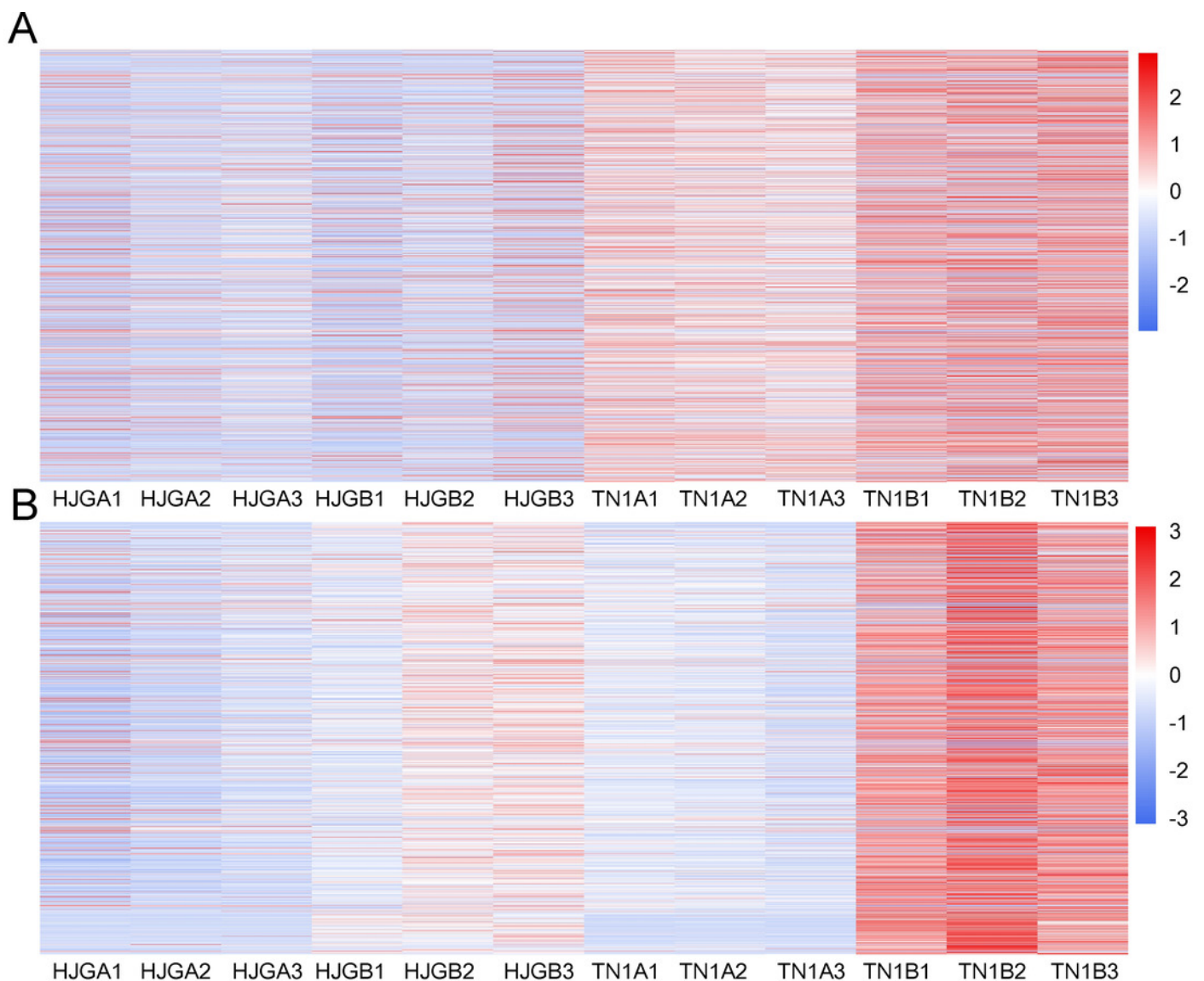


Figure 5

KEGG pathway enrichment in two co-expression modules.

(A) Brown module. (B) Yellow module. The x-axis indicates the enrichment factor; the y-axis indicates the name of pathways. The size of the dots indicate the number of genes in this pathway, and the color of the dots corresponds to different $-\log_{10}$ (correct p value) ranges.

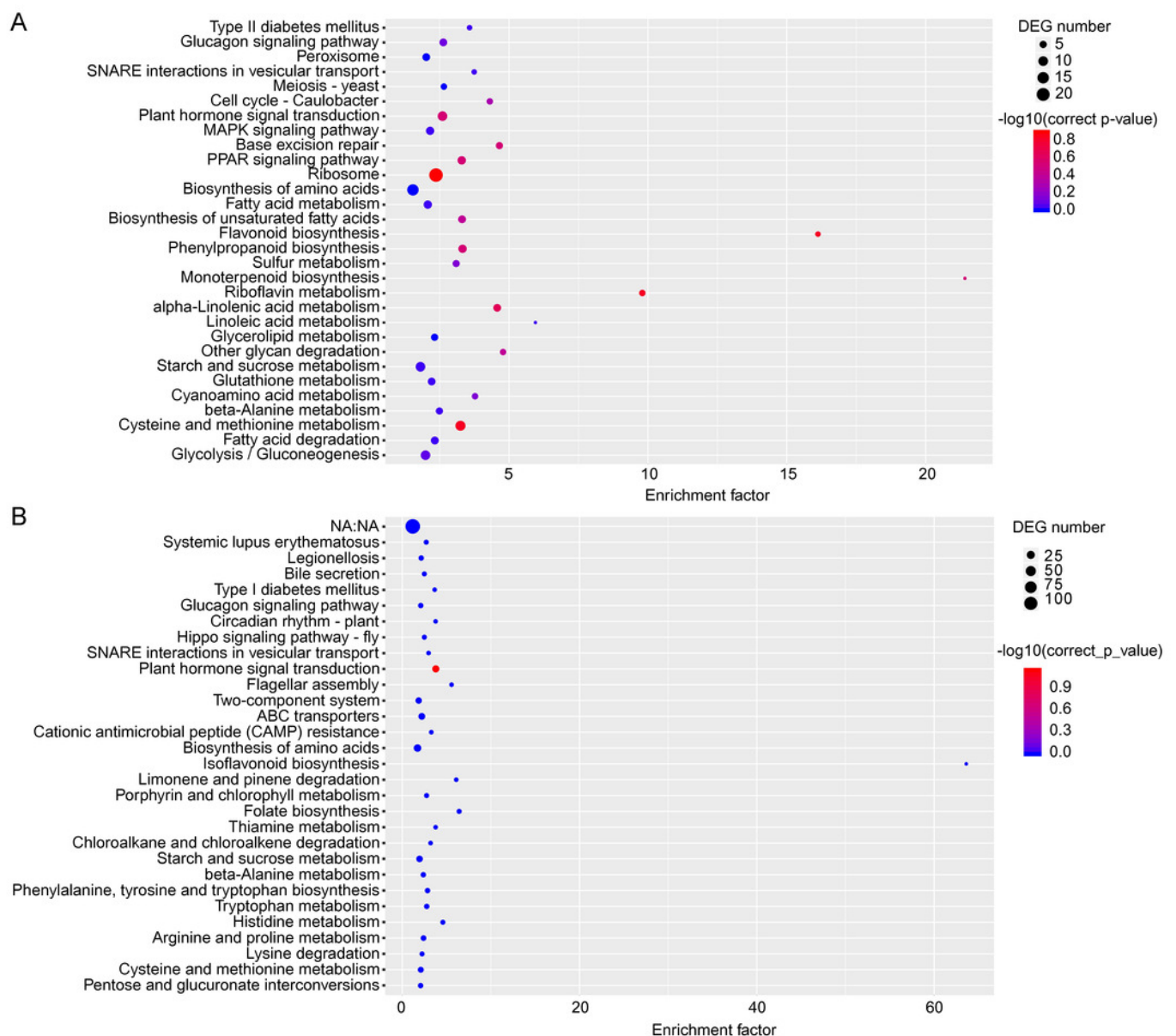


Figure 6

Gene coexpression network related to cold stress.

(A) Gene co-expression network related to cold stress in brown module. (B) Gene co-expression network related to cold stress in yellow module. Red dots represent the hub gene belonging to the co-expression network.

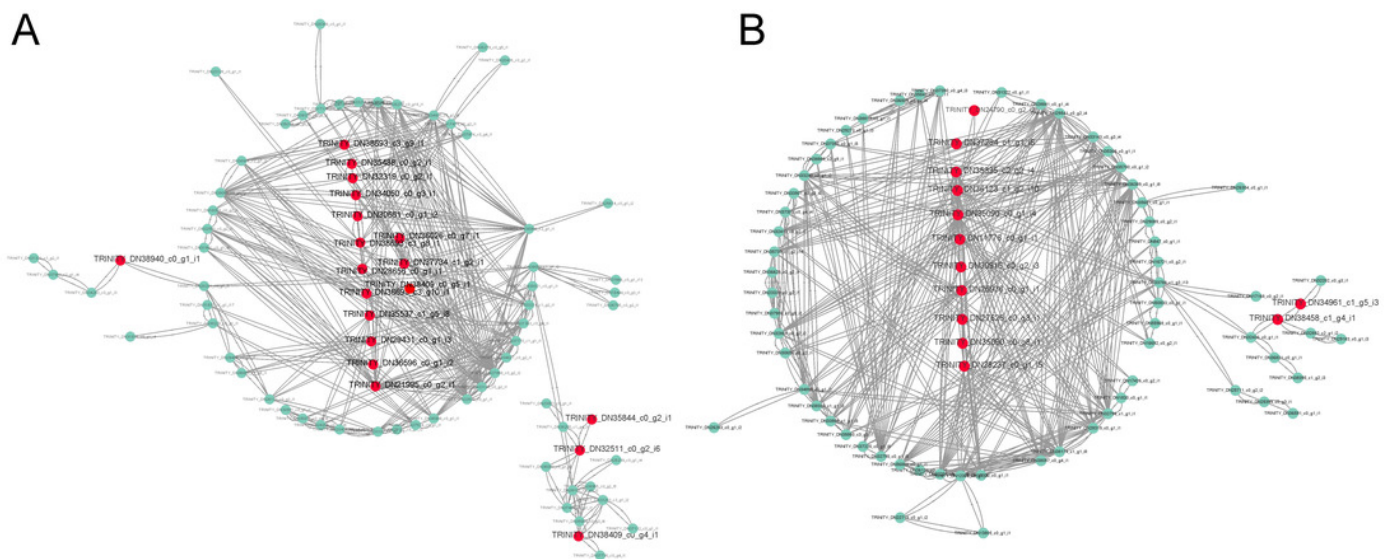


Figure 7

Cold acclimation related genes were validated by RT-qPCR.

The blocks indicate the samples of HJG and TN1 using in RT-qPCR and RNA-seq under cold stress condition. Bars indicate standard deviations of three biological repetitions.

